Journal of Harbin Engineering University
ISSN: 1006-7043

Vol 46 No. 9
September 2025

Hexagonal Microstrip Antenna Array with Enhanced Gain for 28 GHz 5G Applications

[1]Ghizlane Mounir, [2]Jamal El Abbadi

[12]ERSC Research Team, Mohammadia School of Engineering, Mohammed V University in Rabat

Abstract

Millimeter-wave (mmWave) systems operating at 28 GHz encounter substantial propagation losses, making the development of advanced antenna architectures essential. This paper introduces a compact four-element antenna array featuring hexagonal patch elements, designed on a Rogers RT5880 substrate, characterized by a thickness of 0.45 mm, a loss tangent of 0.0009, and a relative permittivity (ε_r) of 2.2. The array delivers a gain of 12 dB and offers a broad impedance bandwidth of 0.87 GHz. Compared to conventional rectangular patch arrays, which typically offer a bandwidth around 0.34 GHz with a slightly higher gain of 13.06 dB, the hexagonal geometry provides a superior trade-off between reduced physical size The simulation results demonstrate effective impedance matching and consistent radiation behavior, making this antenna configuration a strong candidate for integration into 5G mobile platforms and compact base station equipment, where both efficiency and miniaturization are essential.

Keywords: 5G mmWave communications 28 GHz frequency band,antenna array design,hexagonal patch antenna,high-gain microstrip antenna

1. Introduction

Fifth-generation (5G) mobile networks represent a significant advancement in wireless communications, enabling diverse applications such as enhanced mobile broadband (eMBB), massive machine-type communications (mMTC), and ultra-reliable low-latency communications (URLLC) [1]. These technologies are the foundation for emerging innovations including immersive media, smart cities, and autonomous vehicles, demanding high data rates and reliable connectivity [2].

In response to the considerable rise in data traffic and meet the stringent performance requirements of 5G, millimeter-wave (mmWave) frequency bands, particularly the 24–100 GHz range, have become essential. Among these, the 28 GHz band is widely recognized for providing high-capacity channels suitable for next-generation communication services [3]–[5]. However, mmWave signals face several technical challenges, such as severe free-space path loss, atmospheric attenuation, and sensitivity to blockages, which necessitate antenna solutions with compact size, high gain, and wide bandwidth [4]–[6].

Several studies [7]–[13] have explored mmWave antenna design. In our previous work [13] we have developed a four-element rectangular patch array at 28 GHz, achieving a higher gain of 13.06 dB but with a limited bandwidth of 0.34 GHz. In contrast, the present study adopts a hexagonal patch design that offers a significant bandwidth improvement to 0.87 GHz, while maintaining a respectable gain of 12 dB. This trade-off favors wider bandwidth essential for 5G high data rate applications, demonstrating the hexagonal patch's advantage in balancing gain and bandwidth and providing better adaptation to the demands of future wireless communication systems.

In recent years, a variety of antenna architectures has been explored to address mmWave limitations [14]–[19]. Nonetheless, many existing designs face challenges such as restricted bandwidth, suboptimal efficiency, or bulky structures that hinder integration in dense 5G deployments [20]–[24]. To address these challenges, recent research has focused on alternative geometries like circular and hexagonal patches, which offer improved impedance matching and enhanced electromagnetic performance [25]–[31].

The hexagonal patch, in particular, provides a promising balance between electrical performance and physical size. Furthermore, the choice of substrate material greatly influences antenna efficiency. Rogers RT5880, with its low dielectric loss tangent ($\tan\delta$ = 0.0009), has been shown to

outperform traditional materials like Taconic TLC and FR4 in mmWave applications [10], [32].

To address mmWave 5G challenges, this work details the improvement and fine-tuning of Hexagonal antenna array with four elements, designed for 28 GHz operation. The aim is to enhance both bandwidth and gain. Simulation results show that a single hexagonal patch delivers about 6.37 dB gain, rising to roughly 12 dB in the four-element setup. Additionally, this arrangement offers a wider bandwidth compared to conventional rectangular patch designs.

The present work is structured into four main sections: Section II elaborates on the antenna design methodology and computational simulation framework, Section III provides a comprehensive analysis of the results, and Section IV consolidates the principal conclusions while identifying prospective research trajectories for further development

2. Antenna Configuration

2.1Hexagonal Geometry Antenna Element

The designed antenna element (Fig. 1) employs a hexagonal microstrip patch configuration constructed upon a Rogers RT-5880 dielectric substrate characterized by 0.45 mm thickness, dielectric constant (ε_r) of 2.2, and 0.0009 loss tangent. Impedance matching is achieved via an integrated quarter-wavelength transformer. Initial dimensions were computed using transmission line theory fundamentals [8], with optimized parameters documented in Table 1. This hexagonal geometry originates from a circular patch equivalence, where the starting radius (r) was established following reference [8] methodologies.

$$r = \frac{F}{\sqrt{\varepsilon_{eff}}}\left[1 + \left(\frac{2h}{\pi F \varepsilon_{eff}}\right) \times \left(ln\left(\frac{\pi F}{2h}\right) + 1.7726\right)\right] \quad (1)$$

where $F = 8.791\times10^9/f_r$, f_r is the resonant frequency in Hz, ε_{eff} is the effective dielectric constant, and h is the substrate height. The effective dielectric constant ε_{eff} is given by:

$$\varepsilon_{eff} = \frac{\varepsilon_r + 1}{2} + \frac{\varepsilon_r - 1}{2} \times \frac{1}{\sqrt{1 + \frac{12h}{W}}} \quad (2)$$

where W is the width of the microstrip line. The length L_t ou L_q? of the quarter-wavelength transformer used for impedance matching is calculated as:

$$L_t = \frac{\lambda_g}{4} \; ? \quad (3)$$

where the guided wavelength λ_g is expressed by:

$$\lambda_g = \frac{\lambda_0}{\sqrt{\varepsilon_{eff}}} \quad (4)$$

and λ_0 is the free-space wavelength:

$$\lambda_0 = \frac{c}{f_r} \quad (5)$$

with $c = 3 \times 10^8$ m/s.

Full-wave electromagnetic simulation results confirm effective impedance matching at the target frequency of 28 GHz. The reflection coefficient (S11) attains a lowest value of −33.93 dB, indicating minimal return loss and efficient power transfer (see Figure 2). The corresponding impedance bandwidth, defined by the −10 dB threshold, is approximately 1.12 GHz, Encompassing frequencies from 27.48 GHz to 28.6 GHz. In addition, the Voltage Standing Wave Ratio (VSWR) curve presented in Figure 3 shows a minimum value close to 1 at 28 GHz, further confirming optimal impedance matching at the feed point.

The analysis of the antenna's radiation characteristics reveals a realized gain of approximately 6.37 dB at 28 GHz (Fig. 4). Figures 5 and 6 illustrate the 2D radiation patterns in the E-plane (ϕ = 0°) and H-plane (ϕ = 90°), respectively. The measured beamwidths are 80.5° in the ϕ = 0° plane and 98.1° in the ϕ = 90° plane. Polar directivity plots (Figs. 7 and 8) indicate a main lobe at 0° with side lobes of –24 dB for ϕ = 0°, and a main lobe at 8° with side lobes of –14.5 dB for ϕ = 90°. These radiation characteristics demonstrate moderate directivity, low side lobe levels, and adequate beamwidth, confirming the antenna's suitability for 28 GHz millimeter-wave 5G applications.

Table 1. Geometrical Parameters of the Hexagonal Antenna Element

Paramt ers	W_a	W_q	L_q	L_f	W_f	W	L
Values (mm)	1. 72	0. 15	2. 5	2. 05	1. 55	11. 44	11. 99

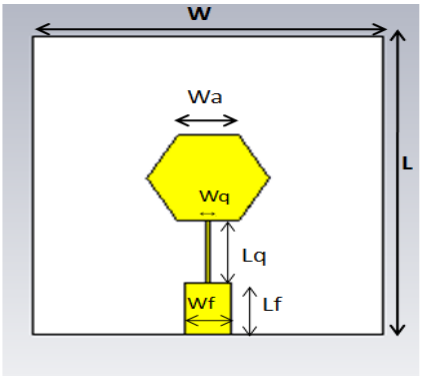

Figure 1. Hexagonal patch antenna design with annotated parameters and feed arrangement.

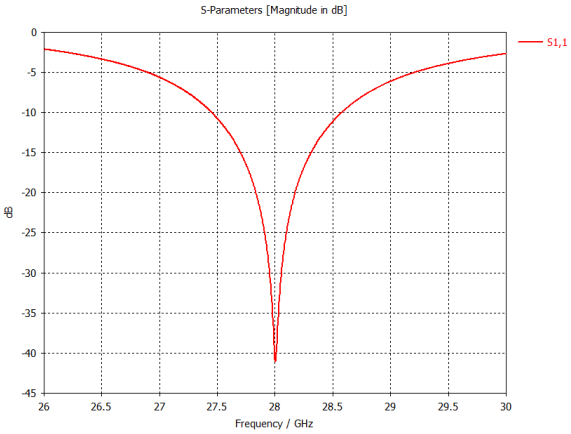

Figure 2. Impedance matching characteristics: Frequency-dependent reflection coefficient (S11) of the hexagonal microstrip antenna

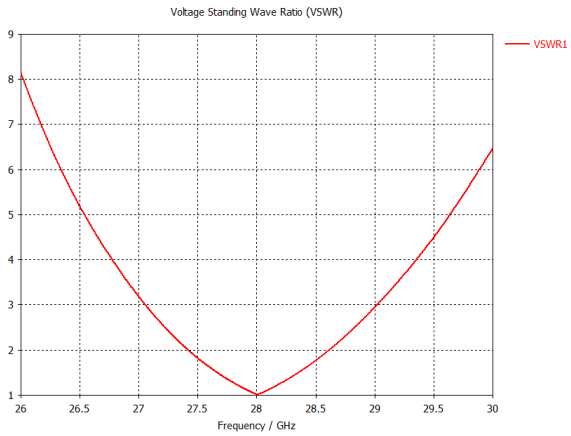

Figure 3. VSWR vs. Frequency Response for the Hexagonal Antenna Element

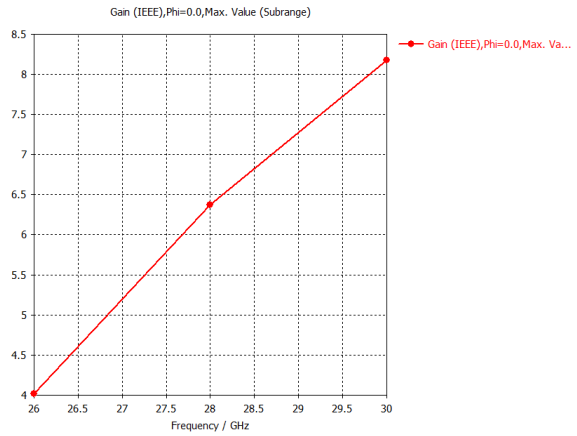

Fig. 4. Antenna gain (dB, vertical axis) versus frequency (GHz, horizontal axis), peaking at 6.37 dBat 28 GHz.

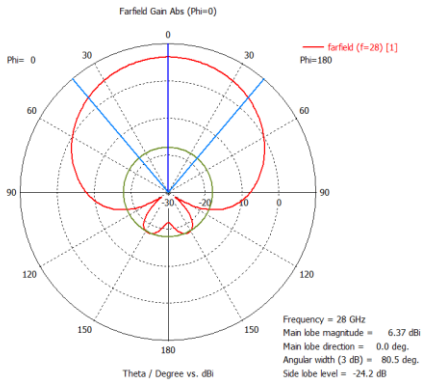

Figure 5. Measured E-plane emission pattern (ϕ = 0°) of the hexagonal patch antenna at 28 GHz...

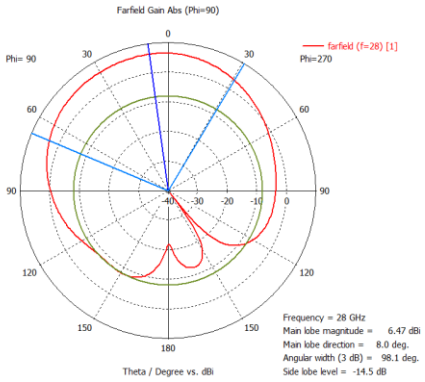

Figure 6. Measured E-plane emission pattern (ϕ =90°) of the hexagonal patch antenna at 28 GHz.

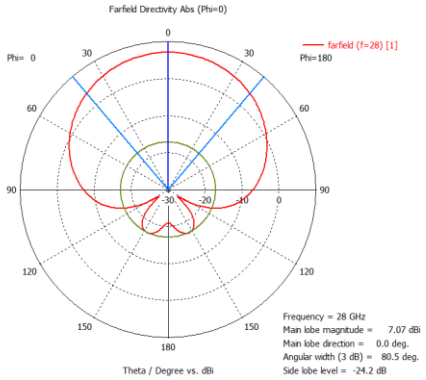

Figure 7. Measured directivity pattern in the H-plane (ϕ = 0°) for the hexagonal patch antenna operating at 28 GHz.

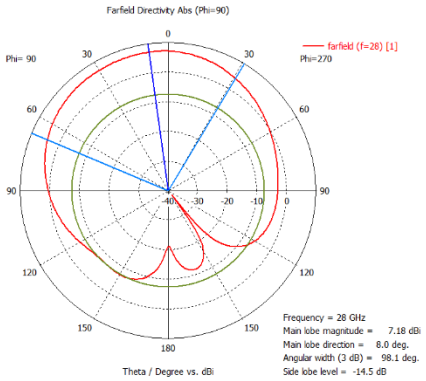

Figure 8. Measured directivity pattern in the H-plane (ϕ = 90°) for the hexagonal patch antenna operating at 28 GHz.

2.2. Hexagonal Antenna Arrays

As illustrated in Figure 1, the standalone hexagonal patch antenna element is engineered for 28 GHz operation, delivering a maximum gain of 6.37 dB, which meets basic 5G specifications. Nevertheless, for mmWave mobile communication systems, which typically demand at least 12 dB gain to ensure consistent signal quality, this performance level may prove inadequate. To overcome this limitation, a phased array architecture is implemented. By integrating multiple hexagonal patches into an organized layout (Figure 9), the total gain is substantially increased. The 1×2 antenna array's design and electromagnetic behavior are thoroughly examined in Figures 10–16, which include S-parameters, voltage standing wave ratio, radiation efficiency, and far-field patterns at 28 GHz for both ϕ = 0° and ϕ = 90° planes. Correspondingly, Figures 18–24 characterize the 1×4 array's performance metrics. In each configuration, precision-engineered power dividers maintain uniform excitation across elements, enhancing radiative properties and facilitating superior beam-steering capabilities.

The detailed specifications of the 1×2 and 1×4 hexagonal arrays are presented in Tables 2 and 3, respectively.

2.2.1. 1×2 Element Hexagonal Antenna Array

The 1×2 hexagonal patch antenna array integrates two identical elements interconnected via a T-junction power divider, ensuring uniform amplitude distribution and phase synchronization. Electromagnetic simulations validate robust impedance matching at 28 GHz, exhibiting a reflection coefficient of −27.96 dB (Figure 10) with a 0.86 GHz operational bandwidth (−10 dB threshold), while the VSWR curve approaches unity (Figure 11), confirming minimal reflections. The array achieves a peak gain of 10.46 dBi (Figure 12), with radiation patterns revealing 32.4° and 28.3° half-power beamwidths in the E-plane (ϕ=0°, Figure 13) and H-plane (ϕ=90°, Figure 14), respectively. The main lobe peaks at 0° azimuth with sidelobe suppression of −11 dB (E-plane) and −1 dB (H-plane) (Figures 15-16), demonstrating directional emission with controlled interference. These characteristics underscore the design's viability for millimeter-wave 5G systems requiring focused radiation and efficient spatial coverage.

Table2. Dimensions of the 1×2 Element Hexagonal Antenna Array

Parameters	wa	Wf	Lf	Wq	Lq	Wq2	Lq2
Values (mm)	1.6	1.55	3.5	0.15	2.7	0.79	1.98

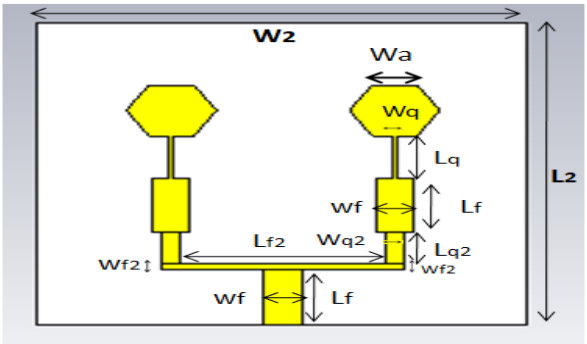

Figure 9. Geometry of the 1×2 Element Hexagonal Antenna Array.

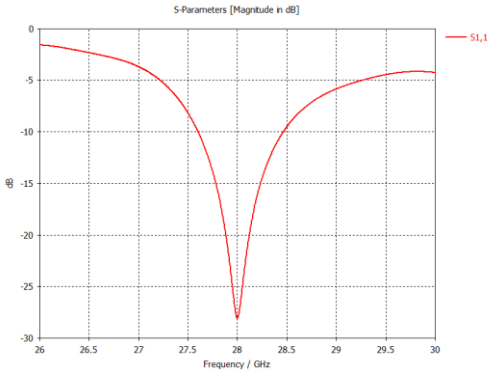

Figure 10. Reflection Coefficient vs. Frequency for the 1×2 Element Hexagonal Antenna Array.

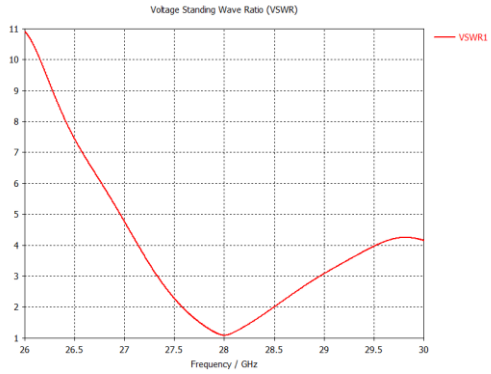

Figure 11. VSWR vs. Frequency Response for the 1×2 Hexagonal Antenna Array.

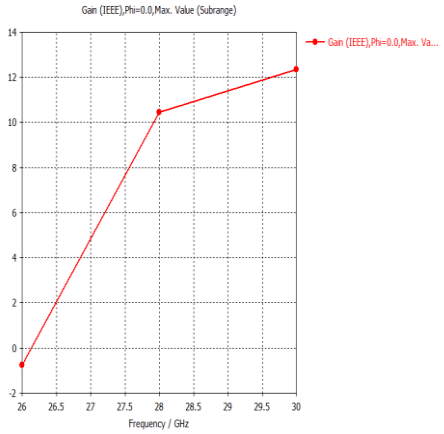

Figure 12. Gain-frequency characteristics of the 1×2 array. The horizontal axis denotes frequency (GHz), while the vertical axis represents gain (dBi). The peak gain of 10.46 dBi is achieved at 28 GHz

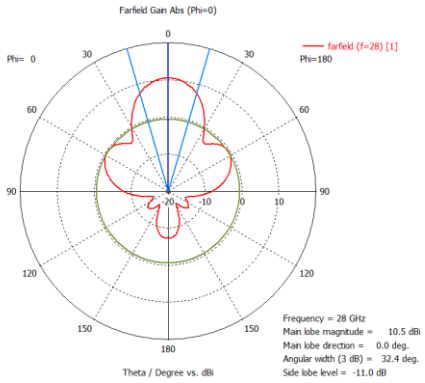

Figure 13. E-plane (ϕ = 0°) radiation characteristics of the 1×2 hexagonal array at 28 GHz.

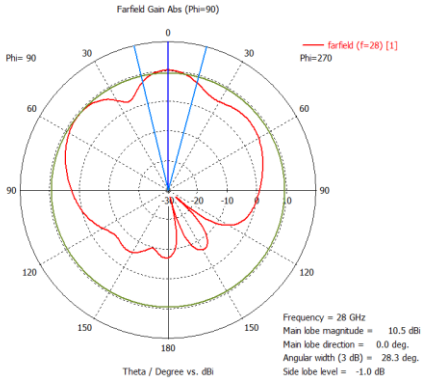

Figure 14. H-plane radiation characteristics (ϕ = 90°) at 28 GHz for 1×2 hexagonal array

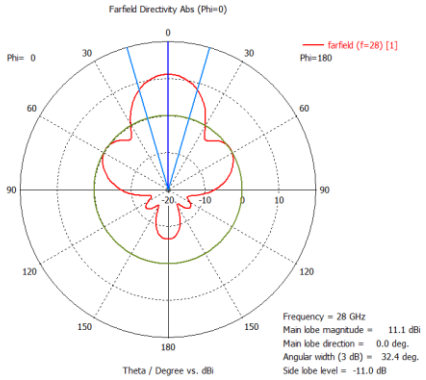

Figure 15. H-plane (ϕ = 0°) directivity characteristics of the 1×2 hexagonal array at 28 GHz.

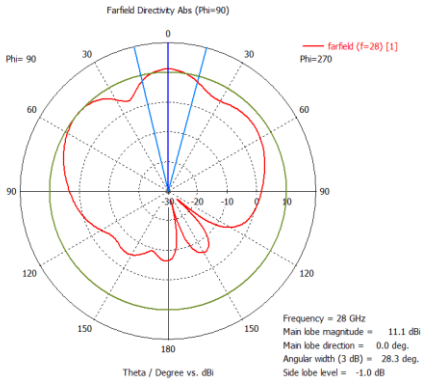

Figure 16. H-plane (ϕ = 90°) directivity characteristics of the 1×2 hexagonal array at 28 GHz.

2.2.2. 1×4 Element Hexagonal Antenna Array

The 1×4 hexagonal antenna array configuration (Figure 17) implements a multi-stage T-junction feed network that interconnects two 1×2 sub-arrays, maintaining consistent amplitude distribution and phase coherence among all radiators. At 28 GHz operation, the array achieves outstanding performance metrics: a return loss of −21.29 dB (Figure 18), 0.87 GHz operational bandwidth (−10 dB criterion), and near-unity VSWR (Figure 19), validating exceptional impedance adaptation. Radiative efficiency peaks at 12 dBi gain (Figure 20), confirming strong suitability for mmWave 5G implementations. Far-field analysis demonstrates focused beams with 15.2° (ϕ=0°, Figure 21) and 35° (ϕ=90°, Figure 22) angular widths. The dominant lobe aligns with 0° azimuth, exhibiting −5.9 dB (ϕ=0°) and −0.5 dB (ϕ=90°) sidelobe magnitudes (Figures 23-24). These characteristics establish the array's capacity for precise directional emission with minimal interference, positioning it as an optimal solution for compact 5G systems requiring stable beam control.

Table 3. Geometric parameters of the 1×4 hexagonal patch antenna array

Parameters	Values (mm)
W_a	1.58
W_f	1.55
L_f	4.5
W_q	0.15
L_q	2.7
W_{q2}	0.79
L_{q2}	1.98
L_{f2}	7.65
W_{f2}	0.4
L_{f3}	16.77
W_3	42.44
L_3	20.46

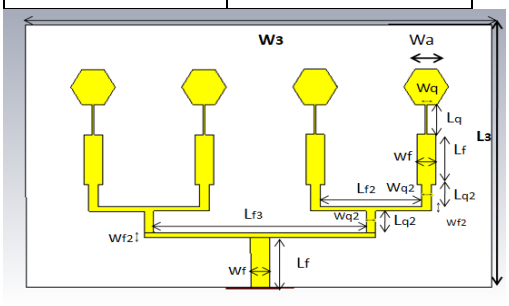

Figure17. Antenna array geometry: 1×4 hexagonal patch configuration with corporate feed structure

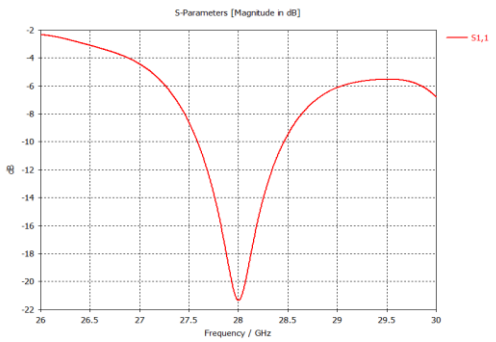

Figure18.Reflection Coefficient vs. Frequency for the 1×4 Element Hexagonal Antenna

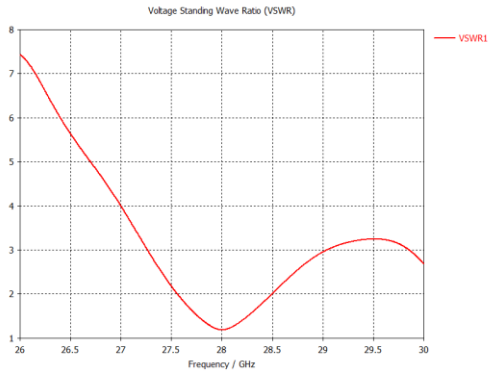

Figure 19. VSWR vs. Frequency Response for the 1×2 Hexagonal Antenna Array

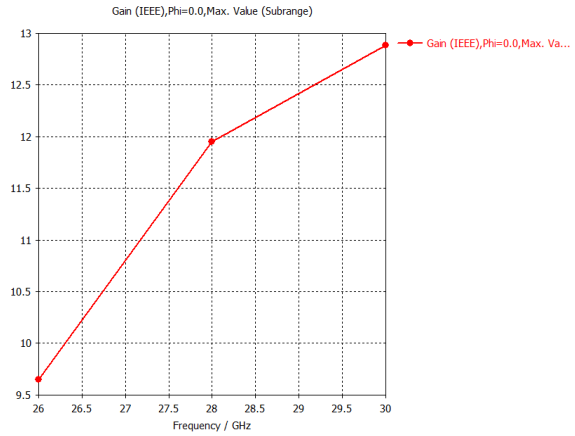

Figure 20 Gain-frequency characteristics (X-axis: Frequency [GHz], Y-axis: Gain [dB]) showing 12 dB peak gain at 28 GHz operation

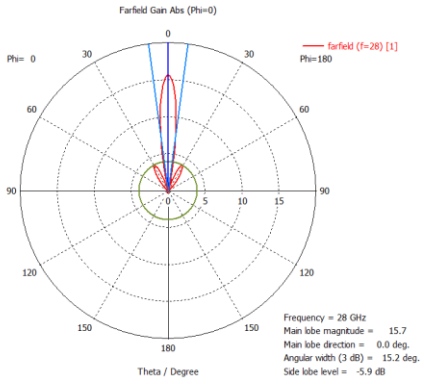

Figure 21. Radiation pattern in the E-plane (ϕ = 0°) of the 1×4 hexagonal patch antenna array operating at 28 GHz.

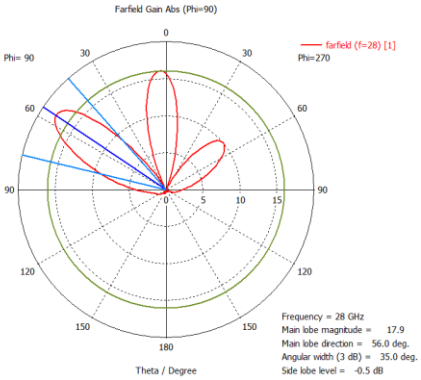

Figure 22. Normalized radiation pattern in the H-plane (ϕ = 90°) for the 1×4 hexagonal antenna array at 28 GHz

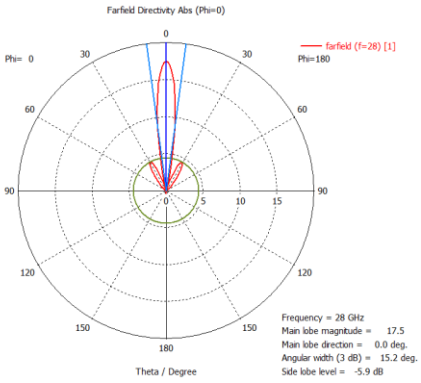

Figure 23. H-plane (ϕ = 0°) directivity characteristics of the 1×2 hexagonal patch array at 28 GHz.

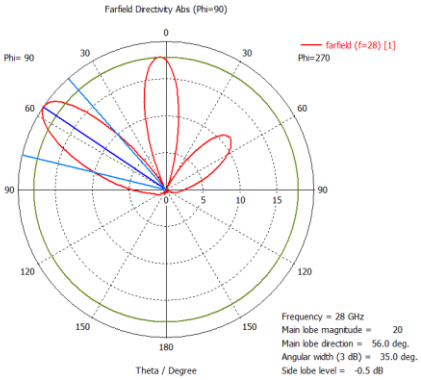

Figure 24. H-plane (ϕ = 90°) directivity characteristics of the 1×2 hexagonal patch array at 28 GHz.

3 Analysis and Discussion of Results

This section presents the key performance results of the proposed hexagonal patch antenna in three configurations: a single element, a 1×2 array, and a 1×4 array. The evaluation is based on simulated performance at 28 GHz, including gain, beamwidth, impedance matching, and radiation characteristics.

A clear improvement in performance is observed as the number of elements increases. The single patch element exhibits a moderate gain of 6.37 dBi with wide beamwidths, indicating suitability for general coverage. Expanding to the 1×2 array significantly enhances the gain to 10.46 dBi, while the beamwidth narrows in both principal planes. The 1×4 array further improves gain to 12 dBi and achieves more focused beams, demonstrating the effectiveness of increasing the array size for higher directivity and better beam control. In terms of impedance matching, all configurations perform well at the target frequency of 28 GHz. The reflection coefficient remains below –20 dB across all cases, ensuring low return loss. Additionally, the VSWR values are close to unity, confirming minimal power mismatch and efficient energy transfer. Radiation pattern analysis reveals progressive improvements in sidelobe suppression as the number of elements increases. The single element exhibits sidelobe levels around –14.5 dB. These are reduced in the 1×2 and 1×4 arrays, reaching –5.9 dB and –0.5 dB respectively, highlighting improved beam shaping and interference rejection. Compared to previous studies on mmWave antenna design [7]–[13], including our own earlier work [13] involving a four-element rectangular patch array at 28 GHz, the proposed hexagonal design offers a more balanced performance. While the previous array achieved a slightly higher gain of 13.06 dBi, its bandwidth was limited to 0.34 GHz. In contrast, the current hexagonal patch array delivers a slightly lower gain of 12 dBi, but with a significantly broader bandwidth of 0.87 GHz. This trade-off favors wider bandwidth, which is essential for high-data-rate 5G applications. The hexagonal configuration thus proves more effective in balancing gain, compactness, and spectral agility, which are critical for future wireless communication systems. Overall, the simulation results confirm that the hexagonal patch antenna, when integrated with a T-junction feed network, provides reliable and scalable performance for millimeter-wave systems. Its compact geometry and consistent enhancement across all key performance indicators make it a promising candidate for 5G front-end integration, where space limitations and strict radiation requirements must be met simultaneously.

Conclusion

This work introduces a compact four-element hexagonal microstrip antenna array optimized for 28 GHz mmWave spectrum used in 5G networks, demonstrating significant performance improvements. It achieves a 12 dB gain and 0.87 GHz bandwidth, outperforming conventional rectangular patch designs. Fabricated using a 0.45 mm Rogers RT5880 substrate, the array benefits from the material's low dielectric loss and high-frequency stability to reduce signal degradation effectively. This configuration offers enhanced main lobe directivity and reduced beamwidth, critical for accurate beam steering and interference mitigation in urban 5G environments. Moreover, it mitigates common mmWave issues like severe path loss and channel variability, boosting spectral efficiency for stable high-speed connectivity. Future work could explore MIMO integration, dual-band functionality, or active phased array compatibility to expand the design's versatility for advanced wireless systems.

Refrences

[1] T. S. Rappaport et al., "Wireless Communications and Applications Above 100 GHz: Opportunities and Challenges for 6G and Beyond," IEEE Access, vol. 7, pp. 78729–78757,2019,doi:10.1109/ACCESS.2019.2921522.

[2] T. S. Rappaport, Y. Xing, G. R. MacCartney, A. F. Molisch, E. Mellios, and J. Zhang, "OverviewofMillimeterWaveCommunications for Fifth-Generation (5G) Wireless Networks—With a Focus on Propagation Models," IEEE Trans. Antennas Propagat., vol. 65, no. 12, pp. 6213–6230, Dec. 2017, doi: 10.1109/TAP.2017.2734243.

[3] R. W. Heath, N. Gonzalez-Prelcic, S. Rangan, W. Roh, and A. M. Sayeed, "An Overview of Signal Processing Techniques for Millimeter Wave MIMO Systems," IEEE J. Sel. Top. Signal Process., vol. 10, no. 3, pp. 436–453, Apr. 2016, doi: 10.1109/JSTSP.2016.2523924.

[4] S. Rana, S. Md. R. Islam, and P. Sikder, "Design and Optimization of Patch Antenna for 5G Applications," in Innovations in Electrical and Electronics Engineering, A. Kalam, S. Mekhilef, and S. S. Williamson, Eds., Singapore: Springer Nature,

2025, pp. 557–573.doi:10.1007/978-981-97-90371_39.

[5] P. Sikder, Md. S. Rana, Md. R. Amin, J. A. Zaman, T. A. Ritu, and M. N. Hasan, "Improving Patch Antenna Performance Utilizing Defected Ground Structure (DGS) for Wireless Applications at Ka-Band," in 2024 15th International Conference on Computing Communication and Networking Technologies (ICCCNT), Jun. 2024, pp. 1–5. doi: 10.1109/ICCCNT61001.2024.10724720.

[6] M. S. Rana et al., "At 28 GHz microstrip patch antenna for wireless applications: a review," TELKOMNIKA(TelecommunicationComputing Electronics and Control), vol. 22, no. 2, Art. no.2,Apr.2024,doi:10.12928/telkomnika.v22i2.25114.

[7] M. S. Rana and M. M. R. Smieee, "Design and analysis of microstrip patch antenna for 5G wireless communication systems," Bulletin of Electrical Engineering and Informatics, vol. 11, no. 6, Art. no. 6, Dec. 2022, doi: 10.11591/eei.v11i6.3955.

[8] C. A. Balanis, Antenna theory: analysis and design, 3rd ed. Hoboken, NJ: John Wiley, 2005.

[9] B. K. Singh, S. Dahiya, and R. Pal, "3D Antenna array for multi-user massive MIMO system to minimize unfavorable propagation," e-Prime - Advances in Electrical Engineering, Electronics and Energy, vol. 8, p. 100571, Jun. 2024, doi: 10.1016/j.prime.2024.100571.

[10] P. Gupta, L. Malviya, and S. V. Charhate, "5G multi-element/port antenna design for wireless applications:a review," Int. J. Microw. Wireless Technol., vol. 11, no. 9, pp. 918–938,Nov.2019,doi: 10.1017/S1759078719000382.

[11] A. Bellekhiri, N. Chahboun, Y. Laaziz, and A. El Oualkadi, "A new design of 5G planar antenna with enhancement of the bandwidth and the gain using metasurface," E3S Web Conf., vol. 351, p. 01054, 2022, doi: 10.1051/e3sconf/202235101054.Bulletin of Electrical Engineering and Informatics, vol. 11, no. 6, Art. no. 6, Dec. 2022, doi: 10.11591/eei.v11i6.3955.

[12] J. Khan, S. Ullah, U. Ali, F. A. Tahir, I. Peter, and L. Matekovits, "Design of a Millimeter-Wave MIMO Antenna Array for 5G Communication Terminals," Sensors, vol. 22, no. 7, p. 2768, Apr. 2022, doi: 10.3390/s22072768.

[13] G. Mounir and J. E. Abbadi, "Antenna Array Design for 28 GHz Millimeter-Wave 5G Communication Systems," in 2024 7th International Conference on Advanced CommunicationTechnologies and Networking (CommNet), Dec. 2024, pp. 1–4. doi: 10.1109/CommNet63022.2024.10793268.

[14] T. Raj, R. Mishra, P. Kumar, and A. Kapoor, "Advances in MIMO Antenna Design for 5G: A Comprehensive Review," Sensors, vol. 23, no. 14,p.6329,Jul. 2023, doi: 10.3390/s23146329.

[15] F. A. Almalki and M. C. Angelides, "An enhanced design of a 5G MIMO antenna for fixed wireless aerial access," Cluster Comput, vol. 25, no. 3, pp. 1591–1606, Jun. 2022, doi: 10.1007/s10586-021-03318-z.

[16] D. Mungur and S. Duraikannan, "Design and Analysis of 28 GHz Millimeter Wave Antenna Array for 5G Communication Systems," vol. 1, no. 3, 2018.

[17] S.-E. Didi, I. Halkhams, M. Fattah, Y. Balboul, S. Mazer, and M. El Bekkali, "Design of a 2×2 dual band 28/38 GHz MIMO antenna in millimeter band for 5G," TELKOMNIKA, vol. 22, no. 2, p. 273, Apr. 2024, doi: 10.12928/telkomnika.v22i2.25268.

[18] S. K. Ibrahim et al., "Design, Challenges and Developments for 5G Massive MIMO Antenna Systems at Sub 6-GHz Band: A Review," Nanomaterials, vol. 13, no. 3, p. 520, Jan. 2023, doi: 10.3390/nano13030520.

[19] Md. S. Rana, T. A. Fahim, S. B. Rana, R. Mahbub, and Md. M. Rahman, "Design, simulation, and analysis of microstrip patch antenna for wireless applications operating at 3.6 GHz," TELKOMNIKA, vol. 21, no. 5, p. 957,Oct.2023,doi:10.12928/telkomnika.v21i5.24813.

[20] J. Li et al., "Dual-Band Eight-Antenna Array Design for MIMO Applications in 5G Mobile Terminals," IEEE Access, vol. 7, pp. 71636–71644,2019,doi:10.1109/ACCESS.2019.2908969.

[21] I. Moumen, M. Elhabchi, M. Nabil Srifi, and R. Touahni, "Metamaterial inspired circular antenna for Bluetooth band integration," TELKOMNIKA, vol.

22, no. 3, p. 510, Jun. 2024, doi: 10.12928/telkomnika.v22i3.25756.

[22] M. A. Khan et al., "mmWave Four-Element MIMO Antenna for Future 5G Systems," Applied Sciences, vol. 12, no. 9, p. 4280, Apr. 2022, doi: 10.3390/app12094280.

[23] N. Chahboun, A. Bellekhiri, J. Zbitou, and Y. Laaziz, "Mutual coupling reduction between antennas array for 5G mobile applications," IJEECS, vol. 34, no. 1, p. 362, Apr. 2024, doi: 10.11591/ijeecs.v34.i1.pp362-369.

[24] H. M. Marhoon, N. Basil, A. R. Ibrahim, and H. A. Abdualnabi, "Simulation and Optimization of Rectangular Microstrip Patch Antenna for Mobile 5G Communications," Jurnal Ilmiah Teknik Elektro Komputer dan Informatika, vol. 8, no. 2, p. 249, Jul. 2022, doi: 10.26555/jiteki.v8i2.21927.

[25] A. Patel et al., "UWB CPW fed 4-port connected ground MIMO antenna for sub-millimeter-wave 5G applications," Alexandria Engineering Journal, vol. 61, no. 9, pp. 6645–6658,Sep.2022,doi:10.1016/j.aej.2021.12.015.

[26] N. R. Palepu, J. Kumar, S. Peddakrishna, and A.Ghosh,"Wideband meander-line-antipodal-vivaldi slot-antenna for millimeter-wave applications," e-Prime - Advances in Electrical Engineering, Electronics and Energy, vol. 9, p. 100641,Sep.2024,doi:10.1016/j.prime.2024.100641.

[27] "Efficient Design of a Multiband Microstrip Series-Fed Array Antenna for 5G Millimeter-WaveApplicationsRequestPDF,"inResearchGate,doi:10.1109/ICECCME57830.2023.10253391.

[28] F. Ouberri, A. Tajmouati, N. Chahboun, L. El Abdellaoui, and M. Latrach, "A novel wideband circularly-polarized microstrip antenna array based on DGS for wireless power transmission," TELKOMNIKA, vol. 20, no. 3, p. 485, Jun. 2022, doi: 10.12928/telkomnika.v20i3.21711.

[29] A. Alkhateeb, S. Alex, P. Varkey, Y. Li, Q. Qu, and D. Tujkovic, "Deep Learning Coordinated Beamforming for Highly-Mobile Millimeter Wave Systems," IEEE Access, vol. 6,pp.37328–37348,2018,doi: 10.1109/ACCESS.2018.2850226..

[30] R. R. Elsharkawy, Khalid. F. A. Hussein, and A. E. Farahat, "Dual-Band (28/38 GHz) Compact MIMO Antenna System for Millimeter-Wave Applications," J Infrared Milli Terahz Waves, vol. 44, no. 11–12, pp. 1016–1037, Dec. 2023, doi: 10.1007/s10762-023-00943-0.

[31] J. Li et al., "Dual-Band Eight-Antenna Array Design for MIMO Applications in 5G Mobile Terminals," IEEE Access, vol. 7, pp. 71636–71644,2019,doi:10.1109/ACCESS.2019.2908969.

[32] D. A. Sehrai et al., "A Novel High Gain Wideband MIMO Antenna for 5G Millimeter Wave Applications," Electronics, vol. 9, no. 6, p.1031,Jun.2020,doi:10.3390/electronics9061031.